Exact non-Markovian master equation for a driven damped two-level system

H. Z. Shen,[1] M. Qin,[1] Xiao-Ming Xiu,[1,2] and X. X. Yi[3,*]

[1]*School of Physics and Optoelectronic Technology, Dalian University of Technology, Dalian 116024, China*
[2]*Department of Physics, College of Mathematics and Physics, Bohai University, Jinzhou 121013, China*
[3]*Center for Quantum Sciences and School of Physics, Northeast Normal University, Changchun 130024, China*

(Received 24 November 2013; published 18 June 2014)

The driven two-level system is a useful model to describe many quantum objects, particularly in quantum information processing. However, the exact master equation for such a system has barely been explored. Making use of the Feynman-Vernon influence functional theory, we derive an exact non-Markovian master equation for the driven two-level system and show the lost feature in the perturbative treatment for this system. The perturbative treatment leads to the time-convolutionless (TCL) and Nakajima-Zwanzig (NZ) master equations. So to this end we derive the TCL and NZ master equations for the system and compare the dynamics given by the three master equations. We find the validity condition for the TCL and NZ master equations. Based on the exact non-Markovian master equation, we analyze the regime of validity for the secular approximation in the time-convolutionless master equation and discuss the leading corrections of the nonsecular terms to the quantum dynamics. Significant effects are found in the dynamics of the driven system.

DOI: 10.1103/PhysRevA.89.062113 PACS number(s): 03.65.Yz, 03.65.Ta, 42.50.Lc

I. INTRODUCTION

The dynamics of open quantum systems [1–3] has attracted much attention and has become active again in recent years due to its possible applications in quantum information science [4–9]. Indeed, the study of the coupled system-environment system is a longstanding endeavor in many fields of physics including quantum optics [10–13], atomic optics [13–17], and condensed matter physics [3,18,19]. The coupling of the system to its environment leads to dissipation and dephasing with flows of energy or information from the system to the environment [2,3]. The backflow of information from the environment to the system determines the Markovianity of the dynamics.

The driven two-level model is available to effectively describe many actual physical systems, for example, a quantum bit in quantum information processing. Thus the theoretical analysis as well as the practical implementation of the driven two-level systems renews the topic. There are several ways to create a driven two-level system (or qubit) by current quantum technologies; each exploits different approaches or works in different quantum systems, for instance, by means of quantum optics and in microscopic quantum objects (electrons, ions, and atoms) in traps, quantum dots, and quantum circuits [20–23]. Different implementations of qubits [24,25] have been subjected to different types of environmental noise [26]; most environments were assumed Markovian [27,28] and the dynamics of the system was studied perturbatively in the literature.

In recent years, there has been increasing interest in developing a non-Markovian generalization for open quantum system theory; several approaches have been formulated in terms of nonlocal time evolutions. Diverse formalisms exist for describing memory effects, including the generalization of the Lindblad master equation from time-independent dissipative rates to time-convoluted kernel functions. A wide class of both phenomenological and theoretical approaches was formulated for building and characterizing this type of master equation, which in turn leads to a completely positive map.

By means of the Feynman-Vernon influence functional theory [29–33], exact master equations describing the general non-Markovian dynamics of a wide range of open quantum systems have been developed recently, e.g., quantum Brownian motion [32,34,35], the single-mode cavity [36] and two entangled cavities [37,38] with vacuum fluctuations, the spin-boson model [39], coupled harmonic oscillators [40–42], a quantum dot in nanostructures [43,44], various nanodevices with a time-dependent external control field [45], nanocavity systems including initial system-reservoir correlations [46], and photonic networks imbedded in photonic crystals [47,48]. However, an exact master equation for driven systems is rare.

The projection operator technique is another way to study the open quantum system; both the time-convolutionless (TCL) [49–51] master equation and the Nakajima-Zwanzig (NZ) [52–54] master equation can be derived by this approach. The NZ approach provides us with a generalized master equation in which the time derivative of the density operator is connected to the past of the reduced density matrix through the convolution of the density operator and an appropriate integral kernel, while the TCL approach leads to a generalized master equation that is local in time. It seems that the NZ approach should be better than the TCL approach in describing the non-Markovian effect since it takes into account the history of the reduced density matrix; however, this is not the case, as we will show later. Examples in [2,55–62] confirm this point, namely, the exact dynamics of the open system can be described via a master equation with a time-dependent decay rate, as in the well-known case of the Hu-Paz-Zhang generalized master equation [2,32].

In the weak-coupling limit, the non-Markovian master equation for a driven two-level system coupled to a bosonic reservoir at zero temperature was derived and discussed in Ref. [61]. This derivation treats the system-environment coupling perturbatively and hence it is available for weak system-environment couplings. In this paper, exploiting the Feynman-Vernon influence theory in the coherent-state

*yixx@nenu.edu.cn

path-integral formalism, we derive an exact non-Markovian master equation for the driven two-level system. The Feynman-Vernon influence theory enables us to treat the environment-system coupling nonperturbatively. The dynamics of the driven open two-level system, going beyond the TCL, NZ, and Markovian approximations, is governed by an effective action associated with the influence functional containing all the influences of the environment on the system. The exact master equation is available to examine the validity of those perturbative approaches applied to the TCL and NZ techniques. We show that the TCL approach works better than the NZ one since the latter does not guarantee the positivity of the density matrix when the correlations in the reservoir become strong, while the former is available for a wider range of values of reservoir memory time.

The remainder of the paper is organized as follows. In Sec. II we introduce a model to describe a driven two-level system subject to the reservoir and give a detailed derivation of the influence functional for the model in the coherent-state representation. In Sec. III an exact non-Markovian master equation describing the evolution of the driven open two-level system is derived. In Sec. IV a derivation of the second-order NZ master equation is presented and the characteristics of the second-order TCL master equation derived in Ref. [2] are discussed; also. we give compare the exact, TCL, and NZ master equations. In Sec. V we investigate the validity of the secular approximation in Markovian and non-Markovian regimes, respectively. Section VI discusses the non-Lorentzian spectrum. A summary is given in Sec. VII.

II. ATOMIC COHERENT-STATE PATH-INTEGRAL APPROACH TO THE DRIVEN OPEN TWO-LEVEL SYSTEM

A. Model Hamiltonian

We start by considering a two-level system with Rabi frequency ω_0 driven by an external laser of frequency ω_L. The two-level atom is embedded in a bosonic reservoir at zero temperature modeled by a set of infinite harmonic oscillators. In a rotating frame, the Hamiltonian of such a system (system plus environment) takes the form

$$H = H_S + H_E + H_I, \tag{1}$$

with

$$\begin{aligned} H_S &= \Delta\sigma_+\sigma_- + \Omega\sigma_x, \\ H_E &= \sum_k \Omega_k a_k^\dagger a_k, \\ H_I &= \sum_k g_k\sigma_+ a_k + \text{H.c.}, \end{aligned} \tag{2}$$

where $\Delta = \omega_0 - \omega_L$, $\Omega_k = \omega_k - \omega_L$, $\sigma_x = \sigma_+ + \sigma_-$, Ω is the driven strength, H.c. stands for Hermitian conjugation, $\sigma_+ = |e\rangle\langle g|$ is the Pauli matrix, and a_k and g_k are the annihilation operator and coupling constant, respectively. In the following we start with this Hamiltonian (1) and derive all the master equations in this paper.

B. Coherent-state representation

The starting point of analysis is to observe that the lowing and raising operators of the atomic transition operators $\sigma_+ = |e\rangle\langle g|$ and $\sigma_- = |g\rangle\langle e|$ satisfy anticommutation rules similar to those of fermions, i.e.,

$$\begin{aligned} \{\sigma_-,\sigma_+\} &= |e\rangle\langle e| + |g\rangle\langle g| \equiv 1, \\ \{\sigma_-,\sigma_-\} &= \{\sigma_+,\sigma_+\} = 0, \end{aligned} \tag{3}$$

where $\{A,B\} = AB + BA$. Identifying the ground state $|g\rangle$ with the fermionic vacuum, we can therefore treat σ_+ and σ_- as fermionic creation and annihilation operators, respectively. Following Ref. [63], we introduce a couple of conjugate Grassmann variables ζ and $\bar\zeta$ imposing standard anticorrelation with the annihilation and creation operators of the system.

Therefore, coherent states are defined as a tensor product of states generated by the exponentiated operation of a creation operator and a suitable label on a chosen fiducial state [29,33,64–66]

$$|\mathbf{z}\rangle = \prod_k |z_k\rangle, \quad |z_k\rangle = \exp(a_k^\dagger z_k)|0_k\rangle, \tag{4}$$

and

$$|\zeta\rangle = \exp(\sigma_+\zeta)|g\rangle. \tag{5}$$

For bosonic coherent states defined in Eq. (4), the label z_k is a complex number and for atomic coherent states defined in Eq. (5), the label ζ is a Grassmannian or anticommuting number. A state of the combined atom-field system can be expanded in a direct product of the coherent state

$$|\mathbf{z}\zeta\rangle = |\mathbf{z}\rangle \otimes |\zeta\rangle. \tag{6}$$

Atomic and bosonic coherent states possess well-known properties such as being nonorthogonal

$$\langle \mathbf{z}|\mathbf{z}'\rangle = \exp\left(\sum_k \bar z_k z_k'\right), \quad \langle\zeta|\zeta'\rangle = \exp(\bar\zeta\zeta'), \tag{7}$$

$$a_k|z_k\rangle = z_k|z_k\rangle, \quad \sigma_-|\zeta\rangle = \zeta|\zeta\rangle, \tag{8}$$

where $\bar z_k$ and $\bar\zeta$ denote the conjugation of z_k and ζ, respectively. Despite their nonorthogonality, both types of coherent states form an overcomplete basis set

$$\int d\varphi(\mathbf{z})|\mathbf{z}\rangle\langle\mathbf{z}| = \int d\varphi(\zeta)|\zeta\rangle\langle\zeta| = 1, \tag{9}$$

where the integral measures are defined by $d\varphi(\mathbf{z}) = \prod_k \exp(-\bar z_k z_k)d^2 z_k/\pi$ and $d\varphi(\zeta) = \exp(-\bar\zeta\zeta)d^2\zeta$. As shown, the bosonic coherent states we use here are not normalized and the normalization factors are moved into the integration measures, which is similar to the Bargmann representation of the complex space. The application of the coherent-state representation makes the evaluation of path integrals extremely simple. In the coherent-state representation, the Hamiltonians of the system, the environment, and the interaction between them are expressed, respectively, as

$$H_S(\bar\zeta,\zeta) = \Delta\bar\zeta\zeta + \Omega(\bar\zeta + \zeta), \quad H_E(\bar{\mathbf{z}},\mathbf{z}) = \sum_k \Omega_k \bar z_k z_k,$$
$$H_I(\bar{\mathbf{z}},\mathbf{z},\bar\zeta,\zeta) = (g_k\bar\zeta z_k + g_k^*\bar z_k\zeta). \tag{10}$$

With this notation, we will present a detailed derivation of the exact master equation for the reduced density matrix of the system in the following sections.

C. Influence functional in coherent-state representation

Explicitly, the density matrix of the whole system (the system plus the environment) obeys the quantum Liouville equation $i\partial\rho_T(t)/\partial t = [H,\rho_T(t)]$, which gives the formal solution

$$\rho_T(t) = \exp(-iHt)\rho_T(0)\exp(iHt). \tag{11}$$

In the coherent-state representation, by use of Eq. (9), $\rho_T(t)$ can be expressed as

$$\begin{aligned}\langle\zeta_f,\mathbf{z}_f|\rho_T(t)|\zeta'_f,\mathbf{z}_f\rangle &= \int d\varphi(\mathbf{z}_i)d\varphi(\zeta_i)d\varphi(\mathbf{z}'_i)d\varphi(\zeta'_i)\langle\zeta_f,\mathbf{z}_f;t|\zeta_i,\mathbf{z}_i;0\rangle\\ &\quad\times\langle\zeta_i,\mathbf{z}_i|\rho_T(0)|\zeta'_i,\mathbf{z}'_i\rangle\langle\zeta'_i,\mathbf{z}'_i;0|\zeta'_f,\mathbf{z}_f;t\rangle.\end{aligned} \tag{12}$$

If we assume that the initial density matrix is factorized into a direct product of the system and the environment state, i.e., $\rho_T(0) = \rho(0)\otimes\rho_E(0)$ [19], the reduced density matrix of the system is then given by

$$\begin{aligned}\rho(\bar{\zeta}_f,\zeta'_f;t) &= \int d\varphi(\mathbf{z}_f)\langle\zeta_f,\mathbf{z}_f|\rho_T(t)|\zeta'_f,\mathbf{z}_f\rangle\\ &= \int d\varphi(\zeta_i)d\varphi(\zeta'_i)\rho(\bar{\zeta}_i,\zeta'_i;0)J(\bar{\zeta}_f,\zeta'_f;t|\bar{\zeta}_i,\zeta'_i;0).\end{aligned} \tag{13}$$

The next task is to determine the effective propagating function for the reduced density matrix [29,30,67]

$$J(\bar{\zeta}_f,\zeta'_f;t|\bar{\zeta}_i,\zeta'_i;0) = \int D^2\zeta D^2\zeta'\exp\{i(S_S[\bar{\zeta},\zeta] - S_S^*[\bar{\zeta}',\zeta'])\}F[\bar{\zeta},\zeta,\bar{\zeta}',\zeta'], \tag{14}$$

where $S_S[\bar{\zeta},\zeta]$ is the action of the system in the atomic coherent-state representation [see Eq. (A2)] and $F[\bar{\zeta},\zeta,\bar{\zeta}',\zeta']$ is the influence functional that takes into account the backaction [in Eq. (A1)] of the environment on the system.

If we assume that the environment is initially at zero temperature, i.e., the initial state of the environment takes the form

$$\rho_E = |0\rangle_{BB}\langle 0|, \tag{15}$$

then the influence functional can be solved exactly to obtain

$$\begin{aligned}F[\bar{\zeta},\zeta,\bar{\zeta}',\zeta'] &= \exp\bigg(\int_{t_0}^t d\tau\int_{t_0}^\tau d\tau'\{f(\tau-\tau')[\bar{\zeta}'(\tau)-\bar{\zeta}(\tau)]\zeta(\tau')\\ &\quad + f^*(\tau-\tau')\bar{\zeta}'(\tau')[\zeta(\tau)-\zeta'(\tau)]\}\bigg),\end{aligned} \tag{16}$$

where

$$f(\tau-\tau') = \sum_k |g_k|^2 e^{-i\Omega_k(\tau-\tau')} = \int d\omega J(\omega)e^{-i(\omega-\omega_L)(\tau-\tau')} \tag{17}$$

is the dissipation-fluctuation kernel. Details of the derivation of Eq. (16) can be found in the Appendix.

III. EXACT NON-MARKOVIAN MASTER EQUATION

We now derive the master equation for the reduced density matrix of the system. Since the effective action after tracing or integrating out the environmental degrees of freedom [i.e., combining Eqs. (14) and (16)] is in a quadratic form of the dynamical variables, the path integral (14) can be calculated exactly by making use of the stationary path method and Gaussian integrals [68,69]. Substituting Eq. (A2) into Eq. (14), we have

$$\begin{aligned}J(\bar{\zeta}_f,\zeta'_f;t|\zeta_i,\bar{\zeta}'_i;0) &= \int D^2\zeta D^2\zeta'\exp\bigg(\tfrac{1}{2}[\bar{\zeta}_f\zeta(t)+\bar{\zeta}(t_0)\zeta_i+\bar{\zeta}'(t)\zeta'_f+\bar{\zeta}'_i\zeta'(t_0)]\\ &\quad -\int_{t_0}^t d\tau\tfrac{1}{2}[\bar{\zeta}\dot{\zeta}-\dot{\bar{\zeta}}\zeta+\dot{\bar{\zeta}}'\zeta'-\bar{\zeta}'\dot{\zeta}']+iH_S(\bar{\zeta},\zeta)\\ &\quad -iH_S(\bar{\zeta}',\zeta')\bigg)F[\bar{\zeta},\zeta,\bar{\zeta}',\zeta'].\end{aligned} \tag{18}$$

To calculate the path integral in Eq. (18), we use the stationary phase method [33,70], which yields the equations of motion

$$\begin{aligned}&\dot{\zeta}(\tau)+i[\Omega+\Delta\zeta(\tau)]+\int_{t_0}^\tau d\tau' f(\tau-\tau')\zeta(\tau')=0,\\ &\dot{\zeta}'(\tau)+i[\Omega+\Delta\zeta'(\tau)]-\int_\tau^t d\tau' f(\tau-\tau')\zeta'(\tau')\\ &\quad+\int_{t_0}^t d\tau' f(\tau-\tau')\zeta(\tau')=0,\end{aligned} \tag{19}$$

subject to the boundary conditions $\zeta(t_0)=\zeta_i$ and $\zeta'(t)=\zeta'_f$, respectively. Here $\bar{\zeta}'(\tau)$ and $\bar{\zeta}(\tau)$ denote the conjugates of $\zeta'(\tau)$ and $\zeta(\tau)$, respectively. The equations for these conjugations can be obtained by first exchanging $\zeta(\tau)$ and $\zeta'(\tau)$ in Eq. (19) and taking then a complex conjugate to these equations. The corresponding boundary conditions are $\bar{\zeta}'(t_0)\equiv\bar{\zeta}'_i$ and $\bar{\zeta}(t)\equiv\bar{\zeta}_f$. With these boundary conditions, we can get the solution of $\zeta(\tau)$ and $\zeta'(\tau)$. For clarity, we illustrate this notation in Fig. 1. Noting $t_0\leqslant\tau\leqslant t$, we keep in mind that

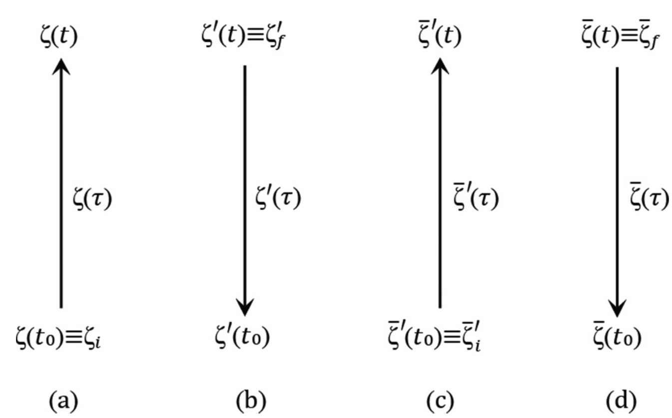

FIG. 1. Schematic illustration of the four independent paths denoted by (a) $\zeta(\tau)$, (b) $\zeta'(\tau)$, (c) $\bar{\zeta}'(\tau)$, and (d) $\bar{\zeta}(\tau)$, respectively.

$\zeta(t)$ in Fig. 1(a) can be obtained by setting $\tau = t$ and $\zeta'(t_0)$ in Fig. 1(b) can be obtained by $\tau = t_0$. Figures 1(c) and 1(d) are similar, namely, $\bar{\zeta}'(t)$ and $\bar{\zeta}'(t_0)$ can be obtained with $\tau = t$ and $\tau = t_0$, respectively.

The solution of the integro-differential equation (19) can be expressed in terms of two complex functions $u(\tau)$ and $u_1(\tau)$ as

$$\zeta'(\tau) = u_1(\tau)[\zeta'_f - \zeta(t)] + \zeta(\tau),$$
$$\zeta(\tau) = u(\tau)\zeta_i + h(\tau). \quad (20)$$

A similar transformation can be written down for their conjugate variables with the exchange of ζ with ζ' for the boundary values $\bar{\zeta}(t) = \bar{\zeta}_f$ and $\bar{\zeta}'(t_0) = \bar{\zeta}'_i$. Substituting Eq. (20) into Eq. (19), we obtain the equations of motion for $u(\tau)$, $u_1(\tau)$, and $h(\tau)$,

$$\dot{u}(\tau) + i\Delta u(\tau) + \int_{t_0}^{\tau} d\tau' f(\tau - \tau')u(\tau') = 0,$$
$$\dot{u}_1(\tau) + i\Delta u_1(\tau) - \int_{\tau}^{t} d\tau' f(\tau - \tau')u_1(\tau') = 0, \quad (21)$$
$$\dot{h}(\tau) + i\Delta h(\tau) + \int_{t_0}^{\tau} d\tau' f(\tau - \tau')h(\tau') = -i\Omega,$$

subject to the boundary conditions $u_1(t) = 1$, $u(t_0) = 1$, and $h(t_0) = 0$ with $t_0 \leqslant \tau$ and $\tau' \leqslant t$. By means of a Laplace transform to Eq. (21), we can easily find that

$$u_1(\tau) = u^*(t - \tau), \quad h(\tau) = -i\Omega \int_{t_0}^{\tau} d\tau' u(\tau - \tau'). \quad (22)$$

Now we set $\tau = t_0$ in the first and $\tau = t$ in the second of Eqs. (20) and $\zeta(t)$ and $\zeta'(t_0)$ can be expressed in terms of the boundary conditions ζ_i and ζ'_f,

$$\zeta(t) = u(t)\zeta_i + h(t),$$
$$\zeta'(t_0) = u^*(t)[\zeta'_f - h(t)] + n(t)\zeta_i, \quad (23)$$

where $n(t) = 1 - |u(t)|^2$. Similarly, $\bar{\zeta}(t_0)$ and $\bar{\zeta}'(t)$ can be obtained by exchanging ζ and ζ' in Eq. (23) and by taking a complex conjugate to these equations. Finally, substituting these results with Eq. (20) into Eq. (18), we obtain the form of the propagating function for the reduced density matrix

$$J(\bar{\zeta}_f, \zeta'_f; t|\zeta_i, \bar{\zeta}'_i; 0) = \exp\{u(t)[\bar{\zeta}_f - h^*(t)]\zeta_i + u^*(t)\bar{\zeta}'_i \times [\zeta'_f - h(t)] + n(t)\bar{\zeta}'_i\zeta_i + h(t)\bar{\zeta}_f + h^*(t)\zeta'_f - |h(t)|^2\}. \quad (24)$$

Note that the preexponential factor in Eq. (24) is one, which is due to the fact that Eq. (24) is the result of integrating out fluctuations around the stationary path. Now we can derive the master equation by computing the time derivative of Eq. (13). First, from Eq. (24), we have the identities

$$\zeta_i J = \frac{1}{u}\left(\frac{\delta J}{\bar{\zeta}_f} - hJ\right), \quad \bar{\zeta}'_i J = \frac{1}{u^*}\left(\frac{\delta J}{\zeta'_f} - h^* J\right), \quad (25)$$

which will be used to remove ζ_i and $\bar{\zeta}'_i$ from the time derivative of J. After taking the time derivative of Eq. (13) and substituting Eqs. (24) and (25) into it, we obtain the evolution equation

$$\frac{\partial\rho(\bar{\zeta}_f, \zeta'_f)}{\partial t} = m\bar{\zeta}_f P_1 + m^*\zeta'_f P_2 - (m + m^*)P_3 + m^*h^*P_1 + mhP_2 - \dot{h}^*P_1 - \dot{h}P_2 - mh\bar{\zeta}_f\rho - m^*h^*\rho\zeta'_f + \dot{h}\bar{\zeta}_f\rho + \dot{h}^*\rho\zeta'_f, \quad (26)$$

where $m(t) \equiv \frac{\dot{u}(t)}{u(t)}$, $P_1 \equiv \frac{\partial\rho}{\partial\bar{\zeta}_f}$, $P_2 \equiv \frac{\partial\rho}{\partial\zeta'_f}$, and $P_3 \equiv \frac{\delta^2\rho}{\partial^2\bar{\zeta}_f\zeta'_f}$. By introducing the functional differential relations in the coherent-state representation [29,43]

$$\bar{\zeta}_f P_1 \leftrightarrow \sigma_+\sigma_-\rho(t), \quad P_2\zeta'_f \leftrightarrow \rho(t)\sigma_+\sigma_-,$$
$$P_3 \leftrightarrow \sigma_-\rho(t)\sigma_+, \quad (27)$$

we arrive at an exact non-Markovian master equation

$$\frac{d\rho(t)}{dt} = -i[H(t), \rho(t)] + \gamma(t)[2\sigma_-\rho(t)\sigma_+ - \{\sigma_+\sigma_-, \rho(t)\}], \quad (28)$$

with the effective Hamiltonian containing the classical driven field

$$H(t) = s(t)\sigma_+\sigma_- + r(t)\sigma_+ + r^*(t)\sigma_-. \quad (29)$$

The renormalized frequency $s(t)$ and the renormalized driving field $r(t)$ are results of the backaction of the environment. The time-dependent dissipative coefficient $\gamma(t)$ describes the dissipative non-Markovian dynamics due to the interaction between the system and environment. All these time-dependent coefficients can be given explicitly,

$$s(t) = \frac{i}{2}[m(t) - \text{c.c.}],$$
$$\gamma(t) = -\frac{1}{2}[m(t) + \text{c.c.}],$$
$$r(t) = i[\dot{h}(t) - h(t)m(t)], \quad (30)$$

where $u(t)$ and $h(t)$ are determined by the integro-differential equations (21). The non-Markovian effect is fully manifested in the integral kernels in Eq. (21), which include the nonlocal time-correlation function $f(t)$ of the environment. The non-Markovian memory effect is coded into the homogenous nonlocal time integrals with the integral kernel. In addition, our derivation of the master equation is fully nonperturbative, which goes beyond the TCL, NZ, and Markovian approximations and includes all effects resulting from the environment-system couplings.

IV. COMPARISON BETWEEN EXACT AND APPROXIMATE MASTER EQUATIONS

A. Nakajima-Zwanzig and time-convolutionless master equations

To derive the second-order perturbative master equation, we first consider the interaction picture, in which the effective Hamiltonian $H_I(t)$ in Eq. (2) can be rewritten as

$$H_I(t) = \sigma_-(t)a^\dagger(t) + \text{H.c.}, \quad (31)$$

where $\sigma_-(t) = U^\dagger(t)\sigma_-U(t)$, $U(t) = e^{-iH_st}$, and $a^\dagger(t) = \sum_k g_k a_k^\dagger e^{i\Omega_k t}$. The density operator $\bar{\rho}_T(t)$ of the whole system including the system and environment satisfies the Liouville equation

$$\dot{\bar{\rho}}_T(t) = -i[H_I(t),\bar{\rho}_T(t)]. \tag{32}$$

Integrating the left- and right-hand sides of Eq. (32), we have

$$\bar{\rho}_T(t) = \bar{\rho}_T(t_0) - i\int_{t_0}^{t} dt'[H_I(t'),\bar{\rho}_T(t')]. \tag{33}$$

Substituting Eq. (33) into Eq. (32), we obtain

$$\dot{\bar{\rho}}_T(t) = -i[H_I(t),\bar{\rho}_T(0)] - \int_{t_0}^{t} dt'[H_I(t),[H_I(t'),\bar{\rho}_T(t')]]. \tag{34}$$

Tracing over the degrees of freedom of the environment, we can obtain the dynamical equation for the system density matrix $\bar{\rho}(t) = \mathrm{Tr}_B\bar{\rho}_T(t)$,

$$\dot{\bar{\rho}}(t) = -i\,\mathrm{Tr}_R[H_I(t),\bar{\rho}_T(t_0)] - \mathrm{Tr}_R\int_{t_0}^{t} dt'[H_I(t),[H_I(t'),\bar{\rho}_T(t')]]. \tag{35}$$

If we apply the Born approximation and assume that the reservoir stays in the vacuum state (15) in the dynamics, we then have

$$\dot{\bar{\rho}}(t) = -\mathrm{Tr}_R\int_{t_0}^{t} dt'[H_I(t),[H_I(t'),\bar{\rho}(t')\otimes\rho_E]]. \tag{36}$$

Notice that

$$\langle a(t)a^{\dagger}(t_1)\rangle = f(t-t_1),$$
$$\langle a^{\dagger}(t)a^{\dagger}(t_1)\rangle = \langle a(t)a(t_1)\rangle = \langle a^{\dagger}(t)a(t_1)\rangle = 0, \tag{37}$$

where $\langle A\rangle = \mathrm{Tr}_B\langle A\rho_E\rangle = \langle 0|A|0\rangle_B$. Substituting Eq. (31) into Eq. (36), we have

$$\dot{\bar{\rho}}(t) = \int_{t_0}^{t} dt' f(t-t')[\sigma_-(t')\bar{\rho}(t'),\sigma_+(t)] + \text{H.c.} \tag{38}$$

By transforming Eq. (38) back into the Schrödinger picture, we obtain

$$\dot{\rho}_{\mathrm{NZ}} = -i[H_S,\rho_{\mathrm{NZ}}(t)] + \int_{t_0}^{t} dt'\{f(t-t')[U(t-t') \times\sigma_-\rho_{\mathrm{NZ}}(t')U^{\dagger}(t-t'),\sigma_+] + \text{H.c.}\}. \tag{39}$$

The non-Markovian master equation (39) is in the standard form of the Nakajima-Zwanzig equation $\dot{\rho}(t) = \int_0^t dt' f(t,t')\rho(t')$ [52,53], where the NZ kernel $f(t,t')$ is of the time translationally invariant form $f(t-t')$.

Note that Eq. (36) is in the form of a delayed integro-differential equation and thus it is a time-nonlocal master equation. It is worth recalling that the other systematically perturbative non-Markovian master equation that is local in time can be derived from the time-convolutionless projection operator formalism [2,55,56]. Now, we discuss the details. Under a similar assumption, i.e., the factorized initial system-reservoir density matrix, the second-order time-convolutionless master equation in the interaction picture can be obtained [2,55–62]

$$\dot{\bar{\rho}}(t) = -\mathrm{Tr}_R\int_{t_0}^{t} dt'[H_I(t),[H_I(t'),\bar{\rho}(t)\otimes\rho_E]]. \tag{40}$$

Substituting Eq. (31) into Eq. (40) and using Eq. (37), we transform Eq. (38) back into the Schrödinger picture and obtain

$$\dot{\rho}_{\mathrm{TCL}} = -i[H_S,\rho_{\mathrm{TCL}}(t)] + \int_{t_0}^{t} dt'\{f(t-t') \times[\sigma_-(t'-t)\rho_{\mathrm{TCL}}(t)\sigma_+ - \sigma_+ \times\sigma_-(t'-t)\rho_{\mathrm{TCL}}(t)] + \text{H.c.}\}. \tag{41}$$

We note here that obtaining the time-convolutionless non-Markovian master equation perturbatively up to second order in the coupling by the use of the time-convolutionless projection operator technique is equivalent to obtaining it by replacing $\bar{\rho}(t')$ with $\bar{\rho}(t)$ in Eq. (36) [2,55–62]. One may wonder if the second-order time-nonlocal master equation (39) is more accurate than the second-order time-convolutionless master equation (41). In the following, using the exact master equation, we show that the TCL approach (41) works better than the NZ one (39) for a wide range of parameters.

B. Comparison to the Nakajima-Zwanzig and time-convolutionless master equations

We now analyze the characteristics of the damped driven two-level systems by comparing the exact dynamics with that from the NZ and TCL master equations. Our purpose is to shed light on the performances of two master equations and to point out their ranges of validity. As stressed in the Introduction, without the exact master equation, it is difficult to examine the range of validity for these master equations.

We assume that the system couples to a reservoir with detuning and the reservoir has a Lorentzian spectral density [2,61,71,72]

$$J(\omega) = \frac{\Gamma}{2\pi}\frac{\lambda^2}{(\omega-\omega_0+\delta)^2+\lambda^2}, \tag{42}$$

where $\delta = \omega_0 - \omega_c$ is the detuning of ω_c to ω_0 and ω_c is the center frequency of the cavity. It is worth noting that the parameter λ defines the spectral width of the reservoir and is connected to the reservoir correlation time $\tau_R = \lambda^{-1}$. The parameter Γ can be shown to be related to the decay of the system in the Markovian limit with a flat spectrum. The relaxation time scale is $\tau_L = \Gamma^{-1}$.

The Markovian dynamics usually describes a situation where the coupling strength between the system and the environment is very weak and the characteristic correlation time τ_R of the environment is sufficiently shorter than that of the system τ_L, i.e.,

$$\tau_R \ll \tau_L, \tag{43}$$

or, equivalently, the spectrum of the reservoir takes the value $J(\omega) = \frac{\Gamma}{2\pi}$, which leads to a Markovian dynamics. The reservoir has no memory effect on the evolution of the system. Then, according to Eq. (17), we have

$$f(t) = \Gamma\delta(t). \tag{44}$$

Substituting Eq. (44) into the first of Eqs. (21), we reduce the solution of $u(t)$ to

$$u(t) = e^{-i\Delta t-(\Gamma/2)t}, \tag{45}$$

i.e., all the coefficients in Eq. (30) are constants,

$$s(t) = \Delta, \quad r(t) = \Omega, \quad \gamma(t) = \Gamma. \tag{46}$$

The exact master equation (28) is then reduced to the Markovian master equation [2,10,73]

$$\begin{aligned}\frac{d\rho(t)}{dt} &= -i[\Delta\sigma_+\sigma_- + \Omega\sigma_x, \rho(t)] \\ &\quad + \frac{\Gamma}{2}[2\sigma_-\rho(t)\sigma_+ - \{\sigma_+\sigma_-, \rho(t)\}],\end{aligned} \tag{47}$$

where the decoherence rates are time independent. This gives the standard Lindblad form for the Markovian dynamics. When

$$\tau_R \geqslant \tau_L \tag{48}$$

is satisfied, the strong non-Markovian effect plays an important role and the dynamics must be described by the exact master equation (28).

Now we calculate the two-time correlation functions $f(t-t')$ by substituting Eq. (42) into Eq. (17),

$$f(t-t') = \tfrac{1}{2}\lambda\Gamma \exp[-(\lambda + i\Delta - i\delta)(t-t')]. \tag{49}$$

It is clear that the bandwidth λ is inversely proportional to the memory time of the reservoir. For this correlation function $f(t-t')$, Eq. (21) can be easily solved by use of Eq. (49); the solution reads

$$u(t) = k(t)\left[\cosh\left(\frac{dt}{2}\right) + \frac{\lambda - i\delta}{d}\sinh\left(\frac{dt}{2}\right)\right], \tag{50}$$

where $k(t) = e^{-(\lambda+2i\Delta-i\delta)t/2}$ and $d = \sqrt{(\lambda - i\delta)^2 - 2\Gamma\lambda}$.

In order to calculate $U(t)$ and $\sigma_-(t)$ in Eqs. (39) and (41), we calculate the eigenstates of the free system Hamiltonian H_S,

$$\begin{aligned}|\phi_{\lambda 1}\rangle &= \frac{1}{\sqrt{2}}(\sqrt{1+\sin\theta}|e\rangle + \sqrt{1-\sin\theta}|g\rangle), \\ |\phi_{\lambda 2}\rangle &= \frac{1}{\sqrt{2}}(\sqrt{1-\sin\theta}|e\rangle - \sqrt{1+\sin\theta}|g\rangle).\end{aligned} \tag{51}$$

The corresponding eigenvalues are $\lambda_1 = (\Delta + W_0)/2$ and $\lambda_2 = (\Delta - W_0)/2$. Here $W_0 = \sqrt{\Delta^2 + 4\Omega^2}$ and $\theta = \arctan(\Delta/2\Omega)$. Straightforward algebra yields

$$\begin{aligned}\sigma_-(t) &= e^{iH_St}\sigma_- e^{-iH_St} = \sum_{j,k=1}^{2}\sigma_{jk}e^{it(\lambda_j-\lambda_k)}|\phi_{\lambda j}\rangle\langle\phi_{\lambda k}|, \\ U(t) &= \sum_{j=1}^{2} e^{i\lambda_j t}|\phi_{\lambda j}\rangle\langle\phi_{\lambda j}|,\end{aligned} \tag{52}$$

where $\sigma_{jk} = \langle\phi_{\lambda j}|\sigma_-|\phi_{\lambda k}\rangle$. Now let us concentrate on the average $\langle\sigma_z\rangle$, i.e., on the probability difference of finding the system in the atomic excited and ground levels. To examine the validity of the two approximate approaches we explore three different regimes by changing the width λ of the Lorentzian spectral density. This investigation will allow us to estimate in which cases the non-Markovian master equations are efficient in the description of the system dynamics.

Figure 2 shows a comparison of the exact, TCL, and NZ master equations with large bandwidth $\lambda = 25\Gamma$. We find that the results given by the TCL master equation (41) and the NZ master equation (39) are in good agreement with those obtained by the exact master equation (28) for any time scales. In this case, both the TCL and NZ master equations give a very good description for the dynamics. They indeed provide us with the same results, which are very close to the Markovian dynamics; see the discussion regarding Eq. (47). In addition, in such cases the use of the TCL master equation, which is

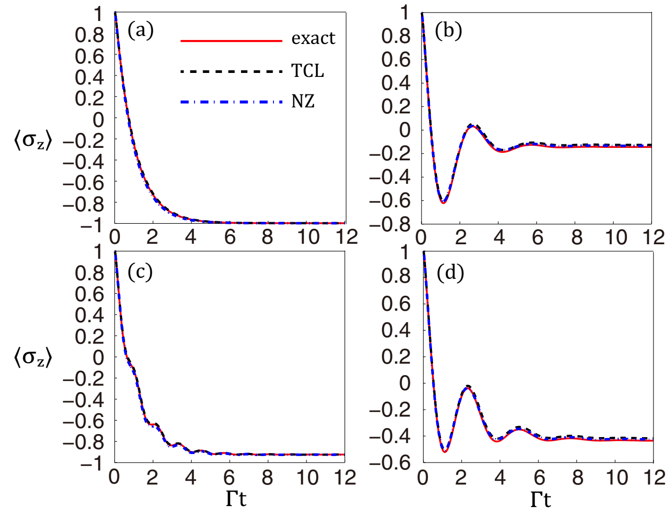

FIG. 2. (Color online) Time evolution of the population difference $\langle\sigma_z\rangle$ for the system initially in the excited state $|e\rangle$ versus the dimensionless parameter Γt. The red solid line, black dashed line, and blue dash-dotted line denote the exact master equation (28), the TCL master equation (41), and the NZ master equation (39), respectively. The width of the Lorentzian spectral density is $\lambda = 25\Gamma$. The other parameters are (a) $\Delta = 0.3\Gamma$, $\Omega = 0.02\Gamma$, and $\delta = 0.01\Gamma$; (b) $\Delta = 0.3\Gamma$, $\Omega = \Gamma$, and $\delta = 0.01\Gamma$; (c) $\Delta = 5\Gamma$, $\Omega = \Gamma$, and $\delta = 0.01\Gamma$; and (d) $\Delta = \Gamma$, $\Omega = \Gamma$, and $\delta = 10\Gamma$.

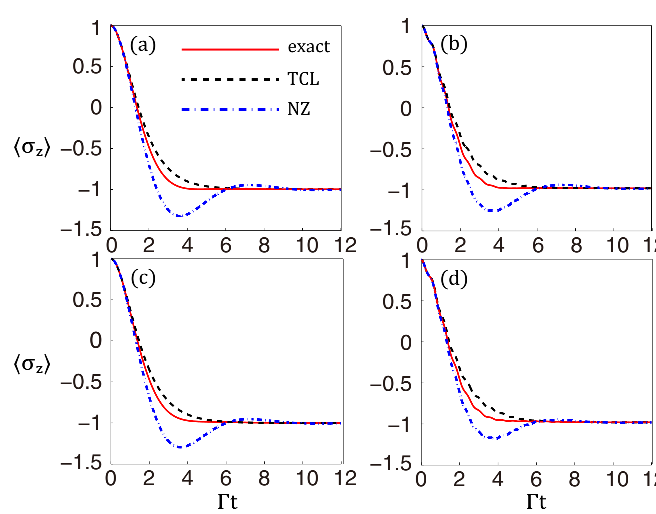

FIG. 3. (Color online) Plot of $\langle\sigma_z\rangle$ versus the dimensionless parameter Γt. The width of the Lorentzian spectrum is $\lambda = \Gamma$. The results are obtained by the exact (red solid line), TCL (black dashed line), and NZ (blue dash-dotted line) solutions. The other parameters are (a) $\Delta = 0.3\Gamma$, $\Omega = 0.02\Gamma$, and $\delta = 0.01\Gamma$; (b) $\Delta = 10\Gamma$, $\Omega = \Gamma$, and $\delta = 0.01\Gamma$; (c) $\Delta = 10\Gamma$, $\Omega = 0.02\Gamma$, and $\delta = 0.2\Gamma$; and (d) $\Delta = 10\Gamma$, $\Omega = \Gamma$, and $\delta = 0.2\Gamma$.

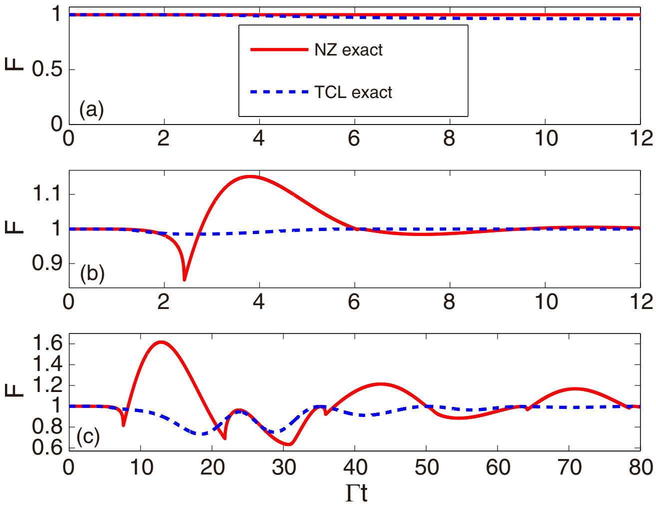

FIG. 4. (Color online) Comparison of the density matrices obtained by solving the TCL and NZ master equations with the one obtained from the exact master equation. We quantify the difference by the fidelity defined by $F(\rho_1,\rho_2) = \mathrm{Tr}\sqrt{\rho_1^{1/2}\rho_2\rho_1^{1/2}}$. The results show that the density matrix given by the TCL master equation is always better than that given by the NZ master equation. The parameters in (a)–(c) are the same as in Figs. 2(a), 3(a), and 5(a), respectively.

easier to solve, might be preferred because it is a time-local first-order differential equation.

We set the same quantity $\lambda = \Gamma$ in Fig. 3. Clearly, the results given by the TCL equation (41) and the NZ equation (39) are in good agreement with those obtained by the exact expression (28) in a short-time scale, but they deviate from each other in a long-time scale. Considering in particular the long-time behavior, the NZ equation leads to a nonphysical result. For times longer than some critical values, the solution for the population difference $\langle\sigma_z\rangle$ cannot represent a physical result because the absolute value of $\langle\sigma_z\rangle$ is larger than 1. We therefore can conclude that for this range of parameters the TCL equation gives a better description of the dynamics because it reflects all the qualitative characteristics of the exact expression.

One may wonder if this observation depends on the quantity plotted. To clarify this point, we plot the fidelity of the density matrix from the exact master equation to these from the TCL and NZ master equations in Fig. 4. The results suggest that the TCL master equation is indeed better than the NZ master equation for a wide range of parameters.

In Fig. 5 we choose the parameter $\lambda = 0.05\Gamma$, which, according to Eq. (49), corresponds to very strong reservoir correlations and a very long memory effect. We find again good agreement between the three approaches in the short-time scale, but in this case the TCL approximation does not work well. The dynamics of the TCL master equation (black dashed line) does not follow the oscillations given by the exact expression (red solid line). The NZ approach has the same problem in that it cannot conserve the positivity of the density matrix (i.e., the absolute value of $\langle\sigma_z\rangle$ exceeds 1). Thus, in this case two approximate methods are not suitable to describe the dynamics of the driven two-level system.

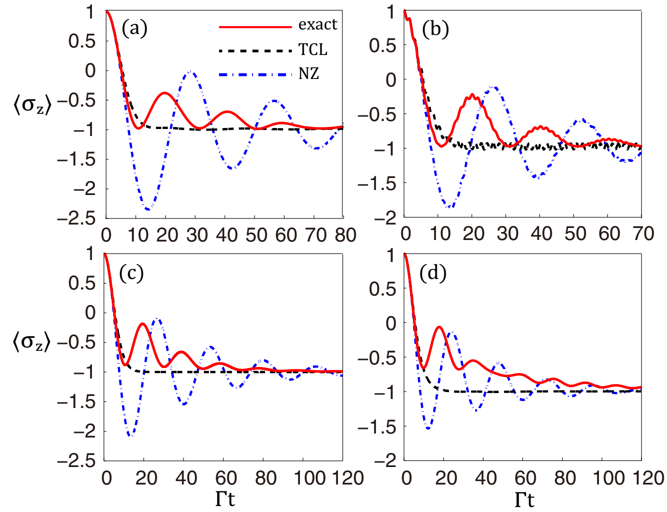

FIG. 5. (Color online) Plot of $\langle\sigma_z\rangle$ versus time Γt. The results are obtained by the exact (red solid line), TCL (black dashed line), and NZ (blue dash-dotted line) solutions. The parameters are (a) $\lambda = 0.05\Gamma$, $\Delta = 0.3\Gamma$, $\Omega = 0.02\Gamma$, and $\delta = 0.01\Gamma$; (b) $\Delta = 3.5\Gamma$, $\Omega = 0.4\Gamma$, and $\delta = 0.01\Gamma$; (c) $\Delta = 10\Gamma$, $\Omega = 0.02\Gamma$, $\delta = 0.08\Gamma$; and (d) $\Delta = 0.3\Gamma$, $\Omega = 0.02\Gamma$, and $\delta = 0.14\Gamma$.

Before closing this section, we discuss the function $f(\tau - \tau')$ in Eq. (17). Concretely, we examine mathematically the validity of extending the lower limit of the integration from 0 to $-\infty$. In the following we will explore three different regimes characterized by the width λ in the spectral density.

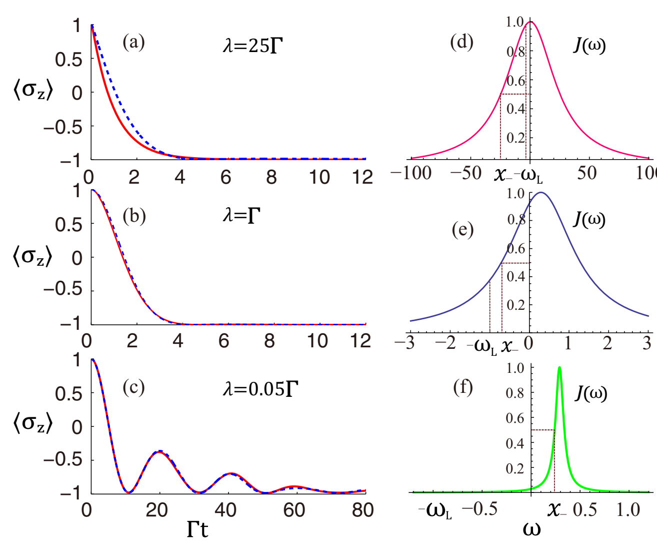

FIG. 6. (Color online) Plot of $\langle\sigma_z\rangle$ given by the exact master equation (28) as a function of time. The purpose of this figure is to show the difference in $\langle\sigma_z\rangle$ caused by different lower limits of the integral of the kernel (53). The red solid and blue dashed lines correspond to lower limits $-\omega_L$ and $-\infty$, respectively. The Lorentzian spectral density $J(\omega)$ (in units of $\Gamma/2\pi$) in (d)–(f) correspond respectively to the results shown in (a)–(c). Here x_- denotes the left location of the half height of the spectral density. The parameters in (a)–(c) are the same as in Figs. 2(a), 3(a), and 5(a), respectively. Notice that $\Delta = \omega_0 - \omega_L = 0.3\Gamma$ in Eq. (2); we set $\omega_0 = 1.3\Gamma$ and $\omega_L = \Gamma$.

In Fig. 6 we show a comparison of the results with two different lower limits in the integration (17) with the spectral density given in Eq. (42); the simulation is performed for the exact dynamics described by Eq. (28). Figure 6(a) is for the integration with a lower limit $-\infty$, which is slightly different from that with a lower limit 0. In Figs. 6(b) and 6(c) the results with a lower limit $-\infty$ are in good agreement with the results obtained with a lower limit 0.

This numerical result can be explained as follows. When we change $\omega \to \omega - \omega_L$, Eq. (17) becomes

$$f(\tau - \tau') = \int_{-\omega_L}^{\infty} d\omega\, J(\omega) e^{-i\omega(\tau-\tau')}, \tag{53}$$

with

$$J(\omega) = \frac{\Gamma}{2\pi} \frac{\lambda^2}{(\omega - \Delta + \delta)^2 + \lambda^2}. \tag{54}$$

This tells us that the frequency ω_L affects only the lower limit of the integral (53) when Δ is fixed. If we define $x_\pm = \Delta - \delta \pm \lambda$ representing the position of the half height of the Lorentzian spectral density (54), we think that the integral of $J(\omega)$ over ω from $-\infty$ to ∞ can be approximately replaced by the same integral but from x_- to x_+. With this approximation, we find that $x_- = -24.71\Gamma$ and $\lambda = 25\Gamma$ in Fig. 6(a). Clearly, x_- is much smaller than $-\omega_L$, thus the integral of $J(\omega)$ over ω from x_- to $-\omega_L$ cannot be ignored [see Fig. 6(d)]. This explains the difference of the two curves in Fig. 6(a). On the contrary, $\lambda = \Gamma$ and $x_- = -0.71\Gamma$ in Fig. 6(b) and $\lambda = 0.05\Gamma$ and $x_- = 0.24\Gamma$ in Fig. 6(c). Here x_- is larger than $-\omega_L$ in both cases of Figs. 6(b) and 6(c). Thus, the integral from $-\omega_L$ to x_- can be ignored [see Figs. 6(e) and 6(f)]. As a result, the two lines in both Figs. 6(b) and 6(c) are in good agreement.

The above discussion suggests that it is reasonable to extend the lower limit of the integral of the Lorentzian spectral $J(\omega)$ from 0 to $-\infty$.

V. VALIDITY OF SECULAR APPROXIMATION IN TIME-CONVOLUTIONLESS MASTER EQUATIONS

Taking advantage of the exact expression for the dissipative dynamics of the open driven two-level system, we have shown that the TCL approach can reveal all the characteristics of the non-Markovian dynamics for a range of parameters much wider than the results that the NZ equation gives. This is physically reasonable since the latter may violate the positivity condition on the density matrix for the reservoir correlations that are not very strong. Therefore, through a comparison with the exact non-Markovian master equation (28), we can investigate the validity of the secular approximation based on the time-convolutionless master equation (41).

We now use the orthonormalized basis (51) and these relations (52) to derive explicitly the time-convolutionless master equations (41) as

$$\dot{\rho} = -i[H_S - H_1, \rho] + D(\rho) + D_1(\rho), \tag{55}$$

with

$$H_1 = g_0^2 Q_0(t) S_z^2 + g_2^2 Q_{+1}(t) S_- S_+ + g_1^2 Q_{-1}(t) S_+ S_-, \tag{56}$$

which describes a small shift in the energy of the two-level system. The above new operators are defined as $S_- = |\phi_{\lambda 2}\rangle\langle\phi_{\lambda 1}|$, $S_+ = |\phi_{\lambda 1}\rangle\langle\phi_{\lambda 2}|$, and $S_z = |\phi_{\lambda 1}\rangle\langle\phi_{\lambda 1}| - |\phi_{\lambda 2}\rangle\langle\phi_{\lambda 2}|$. Then the dissipative superoperator $D(\rho)$ in Eq. (55) can be written in a Lindblad form

$$\begin{aligned} D(\rho) = {} & g_1^2 P_{-1}(t)[2S_-\rho S_+ - \{S_+S_-, \rho\}] \\ & + g_2^2 P_{+1}(t)[2S_+\rho S_- - \{S_-S_+, \rho\}] \\ & + g_0^2 P_0(t)[2S_z\rho S_z - \{S_z^2, \rho\}], \end{aligned} \tag{57}$$

where the coefficients $g_0 = \Omega/W_0$, $g_1 = (W_0 + \Delta)/2W_0$, $g_2 = (W_0 - \Delta)/2W_0$, and $W_0 = \sqrt{\Delta^2 + 4\Omega^2}$. The second dissipator $D_1(\rho)$ in Eq. (55) has a more complicated form and contains the contribution of the so-called nonsecular terms

$$\begin{aligned} D_1(\rho) = {} & g_0 R_0(t)[g_2(S_z\rho S_- - S_-S_z\rho) + g_1(S_+S_z\rho - S_z\rho S_+)] \\ & + g_2 R_1(t)[g_0(S_+\rho S_z - S_zS_+\rho) - g_1 S_+\rho S_+] \\ & + g_1 R_{-1}(t)[g_0(S_zS_-\rho - S_-\rho S_z) - g_2 S_-\rho S_-] + \text{H.c.} \end{aligned} \tag{58}$$

For TCL master equations, the non-Markovian effects are contained in the time-dependent coefficients $P_m(t)$, $Q_m(t)$, and $R_m(t)$, with $m \in \{+,0,-\}$. The time-dependent coefficient reads

$$R_m(t) = \int_0^t dt' \int d\omega\, J(\omega) \exp[i(M_m - \omega)(t - t')], \tag{59}$$

where $M_m = \omega_L - mW_0$. The other coefficients take the forms $P_m(t) = \mathrm{Re}[R_m(t)]$ and $Q_m(t) = -\mathrm{Im}[R_m(t)]$. Conventionally, the nonsecular terms included in the dissipator $D_1(\rho)$ are neglected in the secular approximation. In order to investigate the effects of the nonsecular terms on the non-Markovian dynamics, we focus on two regimes identified by the mutual relationship between the system characteristic time and the reservoir correlation time.

The time-dependent coefficient (59) for the driven two-level system in a Lorentzian reservoir can be calculated explicitly using Eq. (49),

$$R_m(t) = \frac{\Gamma\lambda}{\lambda + iN_m}\{1 - \exp[-(\lambda + iN_m)t]\}, \tag{60}$$

with

$$N_m = \Delta - \delta + mW_0. \tag{61}$$

We can see from Eq. (60) that when $\min(|N_+|,|N_0|,|N_-|) \gg \lambda$, namely, the relaxation time $\tau_R = \lambda^{-1}$ of the reservoir correlation is very large compared to the typical time scale defined as $\tau_S = [\min(|N_+|,|N_0|,|N_-|)]^{-1}$, i.e.,

$$\tau_R \gg \tau_S \tag{62}$$

is satisfied, oscillating terms (58) [those containing $R_m(t)$] may be neglected as t increases since rapid oscillations do not contribute to the dynamics on the time scale of the relaxation. This constitutes the secular approximation.

When

$$\tau_R \leqslant \tau_S, \tag{63}$$

we cannot neglect the nonsecular terms (58) in the master equation (55) in the dynamics of the driven two-level system. Therefore, in this case, we can no longer obtain a simple expression for the system. The master equation of the system is no longer in the time-dependent Lindblad form.

TABLE I. Comparison of regimes of secular and nonsecular approximations in TCL master equations for Markovian and non-Markovian regimes, respectively.

Regime	$\tau_R \gg \tau_S$	$\tau_R \leqslant \tau_S$
Markovian	I	II
$\alpha \to \tau_R \ll \tau_L$	secular	nonsecular
non-Markovian	III	IV
$\beta \to \tau_R \geqslant \tau_L$	secular	nonsecular

Examining Eqs. (43) and (62), we can summarize the comparison of the nonsecular approximation with the secular one in Table I, which shows the validity regimes for secular and nonsecular approximations in the TCL, Markovian, and non-Markovian regimes, respectively.

From Table I we can divide the time-dependent dynamics into two regimes, labeled by α and β, i.e., Markovian and non-Markovian regimes, respectively. In regime α, i.e., the Markovian regime, we can see that the results given by regime I under the secular approximation in the TCL equation (55) are in good agreement with those obtained by the exact master equation (28) when the weak-coupling condition (43) and the secular approximation (62) are simultaneously satisfied [see Figs. 7(a), 7(c), and 7(e)]. When the parameters simultaneously satisfy

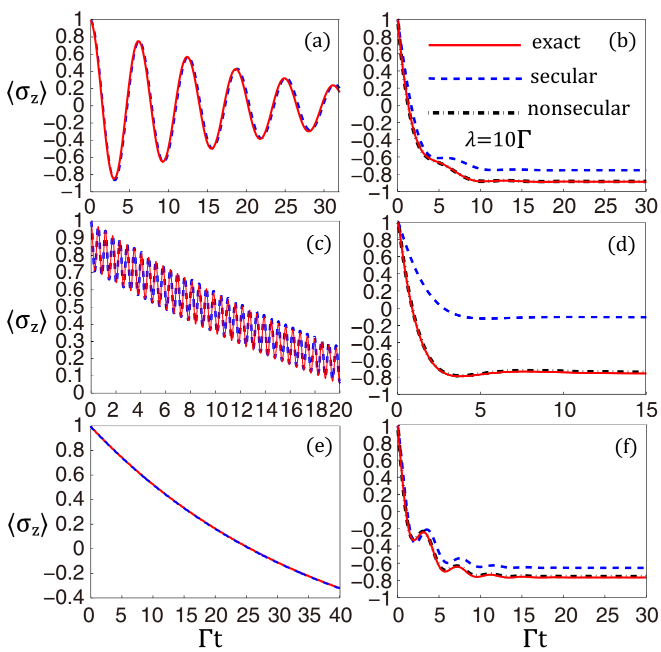

FIG. 7. (Color online) Comparison of the (a), (c), and (e) secular approximation (regime I) and (b), (d), and (f) nonsecular terms (regime II) in the Markovian regime α in Table I. The red solid line, blue dashed line, and black dash-dotted line denote the exact expression (28), the secular approximation (55) neglecting the nonsecular terms (58), and the nonsecular equation (55) containing (58), respectively. The parameters are (a) $\lambda = 10\Gamma$, $\Delta = 0$, $\Omega = 0.5\Gamma$, and $\delta = 40\Gamma$; (b) $\Delta = 0.5\Gamma$, $\Omega = 0.2\Gamma$, and $\delta = 10\Gamma$; (c) $\Delta = 10\Gamma$, $\Omega = 2\Gamma$, and $\delta = 60\Gamma$; (d) $\Delta = 0.1\Gamma$, $\Omega = 0.2\Gamma$, and $\delta = 5\Gamma$; (e) $\Delta = 10\Gamma$, $\Omega = 0.2\Gamma$, and $\delta = 60\Gamma$; and (f) $\Delta = \Gamma$, $\Omega = 0.5\Gamma$, and $\delta = 10\Gamma$.

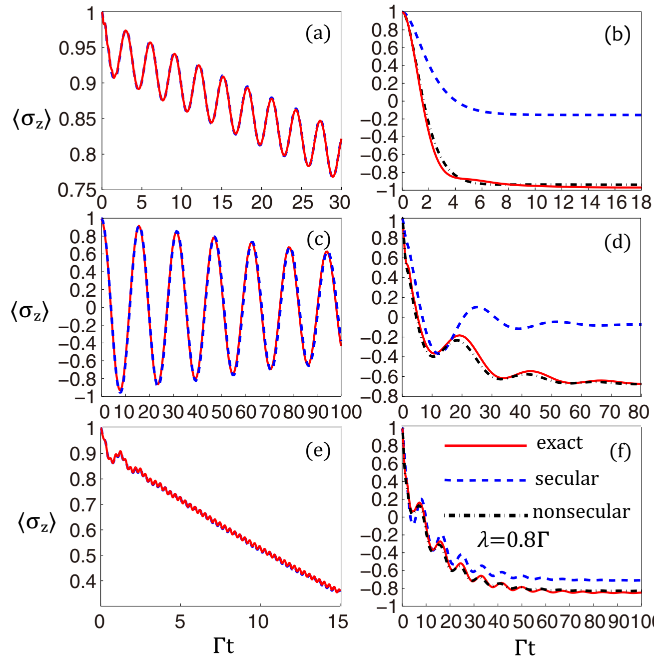

FIG. 8. (Color online) Comparison of the (a), (c), and (e) secular approximation (regime III) with (b), (d), and (f) nonsecular terms (regime IV) in the non-Markovian regime β in Table I. The red solid line, blue dashed line, and black dash-dotted line denote the exact master equation (28), the secular approximation (55) neglecting the nonsecular terms (58), and the nonsecular equation (55) containing (58), respectively. The parameters are (a) $\lambda = 0.8\Gamma$, $\Delta = 2\Gamma$, $\Omega = 0.2\Gamma$, and $\delta = 15\Gamma$; (b) $\Delta = 0.04\Gamma$, $\Omega = 0.06\Gamma$, and $\delta = 0.4\Gamma$; (c) $\Delta = 0$, $\Omega = 0.2\Gamma$, and $\delta = 10\Gamma$; (d) $\Delta = 0.05\Gamma$, $\Omega = 0.1\Gamma$, and $\delta = 1.8\Gamma$; (e) $\Delta = 20\Gamma$, $\Omega = \Gamma$, and $\delta = 5\Gamma$; and (f) $\Delta = 0.5\Gamma$, $\Omega = 0.2\Gamma$, and $\delta = 2.5\Gamma$.

Eqs. (43) and (63) [see Figs. 7(b), 7(d), and 7(f)], i.e., regime II, the dynamics of the TCL master equation (55) involving the nonsecular terms (58) are in good agreement with those obtained by the exact expression (28), but the results obtained by the secular approximation have serious deviations from those obtained by the exact solution (28). This difference comes from the nonsecular terms (58), which are ignored in regime II.

Examining the non-Markovian regime labeled by β in Table I, we find that the results given by the secular approximation (57) in regime III are in good agreement with those obtained by the exact expression (28) when the strong-coupling condition (48) and the secular approximation (62) are simultaneously satisfied [see Figs. 8(a), 8(c), and 8(e)]. When the parameters satisfy simultaneously Eqs. (48) and (63) [see Figs. 8(b), 8(d), and 8(f)], i.e., in regime IV, the dynamics of the TCL master equation (55) involving the nonsecular terms (58) are in good agreement with those obtained by the exact one (28). However, the results obtained by the secular approximation have serious deviations from the exact solution (28). The same observation can be found in regime II.

From Figs. 7 and 8 we can learn that the non-Markovian effect occurs when λ is small. The non-Markovian regime β transits to the Markovian regime α when λ is large. Therefore, by manipulating λ we can control the crossover from non-Markovian to Markovian processes and vice versa. This provides us with a method to manipulate the non-Markovian dynamics in the driven two-level system.

Now we discuss the positivity and complete positivity of the reduced dynamics given by the TCL master equation. The non-Markovian TCL master equation derived in this paper is not of the Lindblad form, even in the secular regime discussed in the present section; therefore, both the positivity and the complete positivity of the reduced dynamics cannot be guaranteed. In other words, the Lindblad-Gorini-Kossakowski-Sudarshan theorem [74,75] that ensures the positivity cannot be satisfied in general, indicating that the dynamics given by the TCL master equation might not be physical for the whole range of parameters.

Nevertheless, the parameters chosen (in fact, it is wide range of parameters) in this paper ensure the positivity of the reduced dynamics given by the TCL master equations. This can be understood as follows. For the driven qubit in the TCL approximation, the necessary and sufficient condition for complete positivity and positivity is given by (for details, see Ref. [61])

$$2\alpha(t) + \beta(t) \geqslant 0, \tag{64}$$

where

$$\alpha(t) = 2\int_0^t d\tau\left[g_1^2 P_{-1}(\tau) + g_2^2 P_{+1}(\tau) + 4g_0^2 P_0(\tau)\right],$$
$$\beta(t) = 4\int_0^t d\tau\left[g_1^2 P_{-1}(\tau) + g_2^2 P_{+1}(\tau)\right]. \tag{65}$$

Returning now to Sec. IV, we stress that the necessary and sufficient condition (64) for complete positivity is satisfied for the parameters chosen in Figs. 3 and 5 (not for a very long time). Therefore, for a wide range of parameters, the complete positivity of the reduced dynamics is guaranteed. Hence our conclusion, i.e., that the TCL equation gives a better description of the dynamics, holds true for a wide range of parameters. It is important to recall that theoretical descriptions of non-Markovian open quantum systems are often based on a series of assumptions and approximations without which it would not be possible to tackle the problem of the description of the dynamics in simple analytic terms. However, those approximations plague almost all approximated reduced dynamics and lead them to break the complete positivity required for reduced dynamics. Therefore, the observation here is available for short times and certain ranges of parameters.

VI. A NON-LORENTZIAN SPECTRUM

Note that the spectral density $J_{\rm SB}(\omega)$ is proportional to the imaginary part of the dynamical susceptibility $\tilde{\chi}(\omega)$ of a damped harmonic oscillator. In this section we present a numerical simulation for $\langle\sigma_z(t)\rangle$ adapting a different spectral density, e.g., the spin-boson spectral density [3,76],

$$J_{\rm SB}(\omega) = \frac{1}{M}\frac{\omega\lambda}{\left(\omega^2-\omega_0^2\right)^2+\omega^2\lambda^2}. \tag{66}$$

In Fig. 9 we plot the time evolution of the population difference $\langle\sigma_z\rangle$ for three typical spectral widths λ. Interestingly, in Fig. 9(a), i.e., for large $\lambda = 25\Gamma$, the population difference $\langle\sigma_z\rangle$ decays monotonically for both the spin-boson and Lorentzian spectral densities; the difference is that the former decays more slowly than the latter. This corresponds to the Markovian case [see the discussion regarding Eq. (47)]. For $\lambda = \Gamma$, small oscillations can be observed in the case with a spin-boson spectral density, while it is not obvious in the case with a Lorentzian spectral density [see Fig. 9(b)]. For small $\lambda = 0.05\Gamma$, oscillations in the population difference can be found in both cases with the spin-boson spectral density and Lorentzian spectral density [see Fig. 9(c)]. These oscillations correspond to a rapid exchange of energy and information between the two-level atom and reservoir.

Spectral density is a key feature for environments. It characterizes the correlation among the particles in the environment and determines the dynamics of an open system, as we have shown in this section.

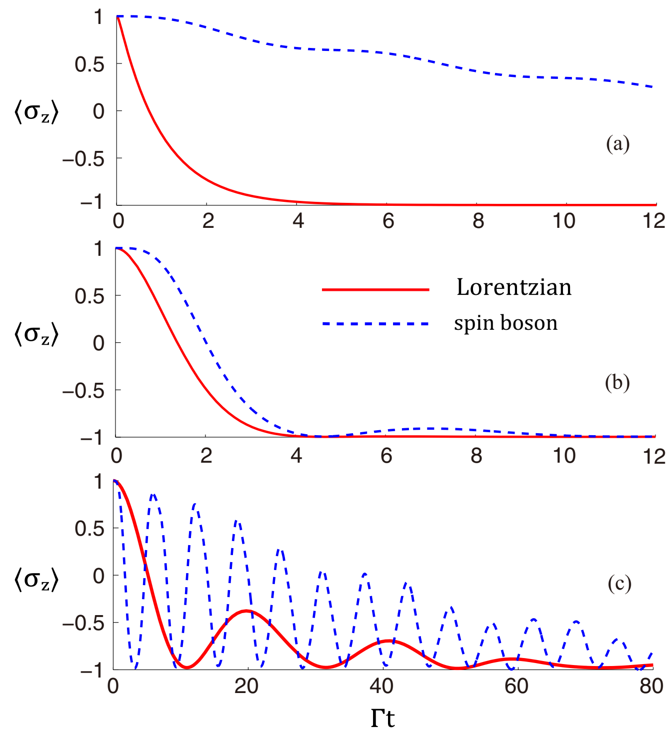

FIG. 9. (Color online) Comparison of the exact dynamics (28) for the Lorentzian (red solid line) and spin-boson (blue dashed line) spectral densities. The parameters in (a)–(c) are the same as in Figs. 2(a), 3(a), and 5(a), respectively. The other parameter is $M = 5\Gamma$.

VII. CONCLUSION

For a driven two-level quantum system, secular and weak-coupling approximations break down when the system-environment coupling varies significantly on the scale of the Rabi frequency. In this paper we avoided these approximations and have studied the non-Markovian dynamics of the driven two-level system coupled to a bosonic reservoir at zero temperature. Making use of the Feynman-Vernon influence functional theory in the coherent-state representation, we derived an exact non-Markovian master equation for the driven two-level system. We compared this exact master equation with the other equations describing non-Markovian dynamics, i.e., the Nakajima-Zwanzig and the time-convolutionless non-Markovian master equations. It was found that the TCL approach is valid for a range of parameters much wider than that for the NZ master equation. This is reasonable since the latter may violate the positivity of the dynamical map when the correlation in the reservoir is strong. By using the exact master equation, we have also given the analytical condition of validity of the secular approximation and shown how it depends on the environmental spectral density. We found that the nonsecular terms have significant corrections to the results obtained by the secular approximation when the relaxation time of the environment is less than or equal to that of the system, i.e., $\tau_R \leqslant \tau_S$.

The limitation of this representation is the state of the bath; here we only consider the bath initially at vacuum. Although the zero-temperature case is problematic for getting reduced dynamics as the bath correlation functions may decay slowly, the zero-temperature reservoir is a good approximation for many problems in physics. For the reservoir initially in a thermal state, the question becomes complicated since the influence functional in the Feynman-Vernon influence functional theory is very involved.

ACKNOWLEDGMENT

This work was supported by the NSF of China under Grant No. 11175032.

APPENDIX: DERIVATION OF THE INFLUENCE FUNCTIONAL

The propagating function controlling the time evolution of the reduced density matrix is given by Eq. (14), where the generalized Feynman-Vernon influence functional is defined by

$$\begin{aligned}F[\bar{\zeta},\zeta,\bar{\zeta}',\zeta'] = &\int d\varphi(\mathbf{z}_f)d\varphi(\mathbf{z}_i)d\varphi(\mathbf{z}_i')D^2\mathbf{z}D^2\mathbf{z}'\\ &\times \rho_E(\bar{\mathbf{z}}_i,\mathbf{z}_i';0)\exp\{i(S_E[\bar{\mathbf{z}},\mathbf{z}]\\ &- S_E^*[\bar{\mathbf{z}}',\mathbf{z}'] + S_I[\bar{\mathbf{z}},\mathbf{z},\bar{\zeta},\zeta] - S_I^*[\bar{\mathbf{z}}',\mathbf{z}',\bar{\zeta}',\zeta'])\},\end{aligned} \tag{A1}$$

where S_S, S_I, and S_E are the actions corresponding to H_S, H_I, and H_E, respectively,

$$\begin{aligned}S_S[\bar{\zeta},\zeta] &= -i[\bar{\zeta}_f\zeta(t) + \bar{\zeta}(t_0)\zeta_i]/2 + \int_{t_0}^t d\tau\{i[\bar{\zeta}(\tau)\dot{\zeta}(\tau)\\ &\quad - \dot{\bar{\zeta}}(\tau)\zeta(\tau)]/2 - H_S(\bar{\zeta},\zeta)\},\\ S_E[\bar{\mathbf{z}},\mathbf{z}] &= \sum_k -i\bar{z}_k z_k(t) + \int_{t_0}^t d\tau[i\bar{z}_k\dot{z}_k(\tau) - H_E(\bar{\mathbf{z}},\mathbf{z})],\\ S_I[\bar{\mathbf{z}},\mathbf{z},\bar{\zeta},\zeta] &= -\int_{t_0}^t d\tau\, H_I[\bar{\mathbf{z}},\mathbf{z},\bar{\zeta},\zeta].\end{aligned} \tag{A2}$$

All the functional integrations are worked out over paths $\bar{\mathbf{z}}(\tau)$, $\mathbf{z}(\tau)$, $\bar{\zeta}(\tau)$, and $\zeta(\tau)$; the end points are $\bar{\mathbf{z}}(t) \equiv \bar{\mathbf{z}}_f$, $\mathbf{z}(t_0) \equiv \mathbf{z}_i$, $\bar{\zeta}(t) \equiv \zeta_f$, and $\zeta(t_0) \equiv \zeta_i$.

Now we can calculate explicitly the influence functional of our model using the coherent-state path-integral formalism. Substituting Eq. (10) into the actions of Eq. (A2), we obtain the explicit form of the propagator. The path integral of the environmental part in the propagator can be exactly done by the stationary phase method [33,70] with the boundary conditions $z_k(t_0) = z_{ki}$ and $\bar{z}_k(t) = \bar{z}_{kf}$. This method needs the equations of motion of the path

$$\dot{z}_k + i\Omega_k z_k = -ig_k^*\zeta, \quad \dot{\bar{z}}_k - i\Omega_k\bar{z}_k = ig_k\bar{\zeta}, \tag{A3}$$

where ζ and $\bar{\zeta}$ are treated as external sources. By formally integrating Eq. (A3), we obtain

$$\begin{aligned}z_k(\tau) &= z_{ki}e^{-i\Omega_k\tau} - ig_k^*\int_0^\tau d\tau' e^{-i\Omega_k(\tau-\tau')}\zeta(\tau'),\\ \bar{z}_k(\tau) &= \bar{z}_{kf}e^{i\Omega_k(\tau-t)} + ig_k\int_\tau^t d\tau' e^{i\Omega_k(\tau-\tau')}\bar{\zeta}(\tau').\end{aligned} \tag{A4}$$

By taking the reservoir to be initially at zero temperature (15), i.e., $\rho_E(\bar{\mathbf{z}}_i,\mathbf{z}_i';0) = 1$, we finally can obtain Eq. (16) after substituting the result and Eq. (A4) into Eq. (A1).

[1] R. Alicki and K. Lendi, *Quantum Dynamical Semigroups and Applications*, 2nd ed., Lecture Notes in Physics Vol. 717 (Springer, Berlin, 2007).

[2] H.-P. Breuer and F. Petruccione, *The Theory of Open Quantum Systems* (Oxford University Press, Oxford, 2002).

[3] U. Weiss, *Quantum Dissipative Systems*, 3rd ed. (World Scientific, Singapore, 2008).

[4] D. P. DiVincenzo, Nature (London) **393**, 113 (1998).

[5] E. Knill, R. Laflamme, and G. J. Milburn, Nature (London) **409**, 46 (2001).

[6] J. I. Cirac, A. K. Ekert, S. F. Huelga, and C. Macchiavello, Phys. Rev. A **59**, 4249 (1999).

[7] D. P. DiVincenzo, Fortschr. Phys. **48**, 771 (2000).

[8] J. I. Cirac, P. Zoller, H. J. Kimble, and H. Mabuchi, Phys. Rev. Lett. **78**, 3221 (1997).

[9] L.-M. Duan, A. Kuzmich, and H. J. Kimble, Phys. Rev. A **67**, 032305 (2003).

[10] C. W. Gardiner and P. Zoller, *Quantum Noise* (Springer, Berlin, 2000).

[11] M. O. Scully and M. S. Zubairy, *Quantum Optics* (Cambridge University Press, Cambridge, 1997).

[12] D. F. Walls and G. J. Milburn, *Quantum Optics* (Springer, Berlin, 1994).

[13] H. J. Carmichael, *An Open Systems Approach to Quantum Optics*, Lecture Notes in Physics Vol. 18 (Springer, Berlin, 1993).

[14] L. Mandel and E. Wolf, *Optical Coherence and Quantum Optics* (Cambridge University Press, Cambridge, 1995).

[15] M. Weissbluth, *Photon-Atom Interactions* (Academic, Boston, 1989).

[16] W. Vogel and D. G. Welsch, *Lectures on Quantum Optics* (Akademie, Berlin, 1994).
[17] G. Compagno, R. Passante, and F. Persico, *Atom-Field Interactions and Dressed Atoms* (Cambridge University Press, Cambridge, 1995).
[18] A. O. Caldeira and A. J. Leggett, Ann. Phys. (N.Y.) **149**, 374 (1983).
[19] A. J. Leggett, S. Chakravarty, A. T. Dorsey, M. P. A. Fisher, A. Garg, and W. Zwerger, Rev. Mod. Phys. **59**, 1 (1987).
[20] J. B. Majer, F. G. Paauw, A. C. J. ter Haar, C. J. P. M. Harmans, and J. E. Mooij, Phys. Rev. Lett. **94**, 090501 (2005).
[21] A. J. Berkley, H. Xu, R. C. Ramos, M. A. Gubrud, F. W. Strauch, P. R. Johnson, J. R. Anderson, A. J. Dragt, C. J. Lobb, and F. C. Wellstood, Science **300**, 1548 (2003).
[22] Y. A. Pashkin, T. Yamamoto, O. Astafiev, Y. Nakamura, D. V. Averin, and J. S. Tsai, Nature (London) **421**, 823 (2003).
[23] B. Bellomo, R. Lo Franco, and G. Compagno, Phys. Rev. Lett. **99**, 160502 (2007).
[24] M. A. Nielsen and I. L. Chuang, *Quantum Computation and Quantum Information* (Cambridge University Press, Cambridge, 2000).
[25] A. Barenco, D. Deutsch, A. Ekert, and R. Jozsa, Phys. Rev. Lett. **74**, 4083 (1995).
[26] M. J. Biercuk, H. Uys, A. P. VanDevender, N. Shiga, W. M. Itano, and J. J. Bollinger, Nature (London) **458**, 996 (2009).
[27] S. Das and G. S. Agarwal, J. Phys. B **42**, 205502 (2009).
[28] I. Sinaysky, F. Petruccione, and D. Burgarth, Phys. Rev. A **78**, 062301 (2008).
[29] C. Anastopoulos and B. L. Hu, Phys. Rev. A **62**, 033821 (2000).
[30] R. P. Feynman and F. L. Vernon, Ann. Phys. (N.Y.) **24**, 118 (1963).
[31] A. O. Caldeira and A. J. Leggett, Physica A **121**, 587 (1983).
[32] B. L. Hu, J. P. Paz, and Y. Zhang, Phys. Rev. D **45**, 2843 (1992).
[33] W. M. Zhang, D. H. Feng, and R. Gilmore, Rev. Mod. Phys. **62**, 867 (1990).
[34] R. Karrlein and H. Grabert, Phys. Rev. E **55**, 153 (1997).
[35] F. Haake and R. Reibold, Phys. Rev. A **32**, 2462 (1985).
[36] J.-H. An, Y. Yeo, and C. H. Oh, Ann. Phys. (N.Y.) **324**, 1737 (2009).
[37] J. H. An and W. M. Zhang, Phys. Rev. A **76**, 042127 (2007).
[38] J. H. An, M. Feng, and W. M. Zhang, Quantum Inf. Comput. **9**, 0317 (2009).
[39] A. Lucke, C. H. Mak, and J. T. Stockburger, J. Chem. Phys. **111**, 10843 (1999).
[40] C.-H. Chou, T. Yu, and B. L. Hu, Phys. Rev. E **77**, 011112 (2008).
[41] J. P. Paz and A. J. Roncaglia, Phys. Rev. Lett. **100**, 220401 (2008).
[42] J. P. Paz and A. J. Roncaglia, Phys. Rev. A **79**, 032102 (2009).
[43] M. W. Y. Tu and W. M. Zhang, Phys. Rev. B **78**, 235311 (2008).
[44] M. W. Y. Tu, M. T. Lee, and W. M. Zhang, Quantum Inf. Process. **8**, 631 (2009).
[45] J. S. Jin, M. T. W. Tu, W. M. Zhang, and Y. J. Yan, New J. Phys. **12**, 083013 (2010).
[46] H. T. Tan and W. M. Zhang, Phys. Rev. A **83**, 032102 (2011).
[47] C. U. Lei and W. M. Zhang, Ann. Phys. (N.Y.) **327**, 1408 (2012).
[48] W.-M. Zhang, P.-Y. Lo, H.-N. Xiong, M. W.-Y. Tu, and F. Nori, Phys. Rev. Lett. **109**, 170402 (2012).
[49] S. Chaturvedi and F. Shibata, Z. Phys. B **35**, 297 (1979).
[50] R. Shibata, Y. Takahashi, and N. Hashitsume, J. Stat. Phys. **17**, 171 (1977).
[51] G. A. Prataviera, A. C. Yoshida, and S. S. Mizrahi, Phys. Rev. A **87**, 043831 (2013).
[52] S. Nakajima, Prog. Theor. Phys. **20**, 948 (1958).
[53] R. Zwanzig, J. Chem. Phys. **33**, 1338 (1960).
[54] J. Zhang, Y.-X. Liu, R.-B. Wu, K. Jacobs, and F. Nori, Phys. Rev. A **87**, 032117 (2013).
[55] H.-P. Breuer, B. Kappler, and F. Petruccione, Phys. Rev. A **59**, 1633 (1999).
[56] Y. J. Yan, Phys. Rev. A **58**, 2721 (1998).
[57] E. Ferraro, M. Scala, R. Migliore, and A. Napoli, Phys. Rev. A **80**, 042112 (2009).
[58] R. X. Xu and Y. J. Yan, J. Chem. Phys. **114**, 3868 (2001).
[59] M. Schröer, U. Kleinekathöfer, and M. Schreiber, J. Chem. Phys. **124**, 084903 (2006).
[60] K.-L. Liu and H.-S. Goan, Phys. Rev. A **76**, 022312 (2007).
[61] P. Haikka and S. Maniscalco, Phys. Rev. A **81**, 052103 (2010).
[62] P. Haikka, Phys. Scr. **T140**, 014047 (2010).
[63] K. E. Cahill and R. J. Glauber, Phys. Rev. A **59**, 1538 (1999).
[64] R. J. Glauber, Phys. Rev. **131**, 2766 (1963).
[65] S. Shresta, C. Anastopoulos, A. Dragulescu, and B. L. Hu, Phys. Rev. A **71**, 022109 (2005).
[66] A. Ghosh, S. S. Sinha, and D. S. Ray, Phys. Rev. E **86**, 011138 (2012).
[67] A. Ishizaki and Y. Tanimura, Chem. Phys. **347**, 185 (2008).
[68] L. D. Faddeev and A. A. Slavnov, *Gauge Fields: Introduction to Quantum Theory* (Benjamin-Cummings, Reading, MA, 1980).
[69] R. P. Feynman and A. R. Hibbs, *Quantum Mechanics and Path Integrals* (McGraw-Hill, New York, 1965).
[70] J. R. Klauder, Phys. Rev. D **19**, 2349 (1979).
[71] J.-G. Li, J. Zou, and B. Shao, Phys. Rev. A **81**, 062124 (2010).
[72] H. Z. Shen, M. Qin, and X. X. Yi, Phys. Rev. A **88**, 033835 (2013).
[73] V. N. Shatokhin and S. Ya. Kilin, Opt. Commun. **174**, 157 (2000).
[74] G. Lindblad, Commun. Math. Phys. **48**, 119 (1976).
[75] V. Gorini, A. Kossakowski, and E. Sudarshan, J. Math. Phys. **17**, 821 (1976).
[76] M. Thoss, H. Wang, and W. H. Miller, J. Chem. Phys. **115**, 2991 (2001).